PROCEEDINGS, 41st Workshop on Geothermal Reservoir Engineering
Stanford University, Stanford, California, February 22-24, 2016
SGP-TR-209

Effects of Observation Well Location in Lumped Parameter Models

Ufuk Ozturk, Omer Inanc Tureyen and Abdurrahman Satman

Istanbul Technical University, ITU Petrol ve Dogal Gaz Muh. Bol., Maslak, Istanbul, TURKEY

e-mail: ufukoztrk@gmail.com, inanct@itu.edu.tr and mdsatman@itu.edu.tr

Keywords: Lumped parameter modeling, Errors

ABSTRACT

Lumped Parameter modeling is used as a widespread tool for predicting the performance of a geothermal reservoir. Being a simple and an efficient method lumped parameter models can give performance predictions in a short time. By history matching the past data, the behavior of the reservoir can be characterized, which is done especially by determining recharge indices and storage capacities of each tank that the geothermal system is represented by. Hence, if error is introduced to the average reservoir pressure and/or temperature values, these errors will propagate into the parameters that will be estimated. Having estimated the parameters with error will lead to an incorrect future performance prediction which would then lead to poor reservoir management. In this study, for the liquid dominated isothermal geothermal reservoirs containing single-phase liquid water, the errors made in estimation of the model parameters, caused by the errors in the average reservoir pressure inputs, are characterized. First of all, for the synthetic data generation, a 2D numerical model is generated. Then lumped parameter models are used to history match to the synthetic data in order to obtain the recharge index and storage capacity values for the representing lumped parameter model. By using the inverse model and numerical model, errors are investigated. Based on the results, the reservoir systems that have aquifer connection will lead to drastic errors if the proper observation well is not chosen.

1. INTRODUCTION

Reservoir modeling is a must for developing geothermal systems in an efficient manner. The reservoir engineer together with the subsurface team tries to predict the geothermal reservoir parameters. As new wells are drilled or operations are made, new production data are acquired and clues for a more accurate model are obtained. Two conventional methods are used for modeling geothermal reservoirs. First one is numerical modeling. Second one is lumped parameter modeling.

In the numerical models, various numbers of grids, which possibly but not necessarily have different properties, are used to model the producing reservoir. Conservation equations are solved for each grid block to obtain the performance of the geothermal system. The types of equations solved by these models are energy and mass balances. The geological complexity of geothermal systems represent yet another challenge for representation in numerical models. In order to represent these complex geological features, many numbers of grids must be used leading to very long run times. Furthermore, such large models will usually require large amounts of data to be input. The long run times would especially present a problem for history matching, since the model would need to be run many numbers of times.

In lumped parameter modeling, the geothermal system is modeled using “tanks”. Tanks are basically control volumes where conservation equations are applied on. Various numbers of tanks can be used to model the geothermal system. Each tank would then represent a specific component of the geothermal system such as the reservoir, aquifer and etc. Lumped parameter models provide an attractive alternative. First of all they are extremely fast since the number of parameters associated with these models is much smaller when compared with numerical models. During the history matching process, instead of matching the behavior of individual wells, observation well pressures (which are believed to represent average reservoir pressures) are used. With lumped parameter models, average pressure and/or temperature performance predictions can be made.

Lumped parameter modeling was first developed by Whiting and Ramey (1969) for reservoirs both considering mass and energy balance. Later on Castanier et al. (1980) developed an analytical model for simulating the geothermal reservoirs. This method could be used for all liquid, all steam and two-phase cases in radial geometry.

Olsen (1984), in his study presented the ways of modeling the liquid-dominated geothermal reservoirs and matched the historical data for Svartsengi geothermal field in Iceland. Also, Axelsson (1989) used lumped parameter modeling to simulate some of the low temperature geothermal fields located in Iceland. Later Sarak et al. (2005) provided analytical equations for lumped parameter models and studied different schemes of lumped parameter models to match the Laugarnes field in Iceland and Balcova-Narlidere field in Turkey. Both Axelsson (1989) and Sarak et al.(2005) assume isothermal systems.

Alkan and Satman (1990) presented a model for the reservoirs involving carbon dioxide. Onur et al. (2008) developed a non-isothermal approach to the lumped parameter modeling both using energy and mass balance. Later, Tureyen et al. (2009) generalized this study to multiple tanks. However, both of the studies consider only heat flow by way of convection between the tanks. The first study including conductive heat flow between the tanks was developed by Tureyen & Akyapı (2011).

In this study, a 2D isothermal numerical model is developed for a single-phase liquid water system. The first part of the paper presents a brief theory for the numerical model developed. Later, a brief explanation of the inverse model is given. The developed inverse model has the capability to determine the storage capacity and recharge index values of a lumped parameter model by way of history matching to observed pressure data. The inverse and numerical models are used to investigate the errors for the different reservoir systems. The outcomes of the simulation runs are discussed in the last part of the paper.

2. NUMERICAL MODEL

In this study the reservoir system is assumed to be isothermal and the model used is based on the mass balance of a single phase fluid. The reservoir system consists of N_t number of grids. Mass balance is applied on each grid block and solved simultaneously for each time step. Figure 1 shows the grid system.

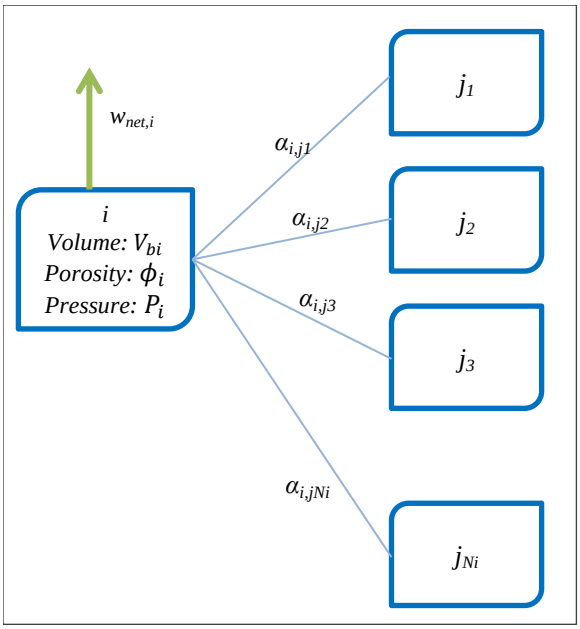

Figure 1 : Schematic of the grid system.

As it can easily be seen grid *i* makes connection with an arbitrary N_i number of grids. For the above case, V_{bi} (m^3) is the bulk volume, ϕ_i is the porosity, p_i (bar) is the pressure, ρ_w (kg/m^3) is the density of the water in the system and c_t (1/bar) is the total compressibility which is considered to be independent of pressure. The mass balance for grid block *i* can be written as given in Eq. 1.

$$(\text{Net rate of accumulation in grid i}) = (\text{Net mass production rate}) + (\text{Net mass rate from connecting tanks}) \quad (1)$$

Net accumulation in grid *i* can be calculated with the following equation:

$$(w_{acc})_i = \kappa_i \frac{\partial p_i(t)}{\partial t} \quad (2)$$

where κ_i (kg/bar) is the storage capacity of grid *i* and calculated with $\kappa_i = (V_{bi}\phi\rho_w c_t)_i$. Mass rate to/from connected grids can be calculated as follows:

$$(\text{Net mass rate from connecting tanks}) = \sum_{l=1}^{N_i} w_{i,j_l} \quad (3)$$

where w_{i,j_l} is the mass flow rate to/from grid j_1 to/from grid *i* and calculated with the Schilthuis's (1936) steady state model:

$$w_{i,j_1} = \alpha_{i,j_l}(p_{j_l} - p_i) \quad (4)$$

where α_{i,j_l} (kg/bar-s) is the recharge index between grid *i* and j_1. Combining Eq. 3 and Eq. 4 the mass balance for grid *i* can be written as:

$$\kappa_i \frac{\partial p_i}{\partial t} = \sum_{l=1}^{N_i} \alpha_{i,j_l} \left(p_{j_l} - p_i \right) - w_{net,i} \qquad (5)$$

Using a finite difference scheme for the time derivatives and a fully implicit treatment of pressures the equation will become as given in Eq. 6.

$$\sum_{l=1}^{N_i} \alpha_{i,j_l} p_{j_l}^{n+1} + \left(\sum_{l=1}^{N_i} \alpha_{i,j_l} - \frac{\kappa_i}{\Delta t} \right) p_i^{n+1} = - \frac{\kappa_i p_i^{n}}{\Delta t} + w_{net,i}^{n+1} \qquad (6)$$

In the above formula *n* and *n+1* represent the time steps. The above equation is solved for all grid blocks and as a result the pressures of each grid block are obtained.

3. INVERSE MODEL

An inverse model is developed that history matches to the pressure data and determines parameters such as the recharge indices and storage capacities. Such an approach using lumped parameter modeling is described in detail in Sarak (2004). Basically we apply a least squares type of an approach. Here, for simplicity we use a non-weighted least squares method.

In nonlinear optimization problem a least-squares objective function *(O)* is minimized. The objective function calculates the sum of the squares of the differences with the observations and the model outputs as shown in Eq. 7.

$$O(\mathbf{x}) = \sum_{j=1}^{M} \left[f(t_j, \mathbf{x}) - y(t_j) \right]^2 \qquad (7)$$

where $\mathbf{x} = (\boldsymbol{\alpha}, \boldsymbol{\kappa})$, *M* represents the number of observations, *t* is the time in which observations are made and $y(t)$ are the observation for the given time *t*. $f(t, \mathbf{x})$ is the model outputs. The above objective function is minimized by using Levenberg-Marquardt method which is an iterative method, starting with the initial guess for the model parameters as described in More (1978). After convergence the root mean square error (RMS) value is calculated by using the following formula:

$$RMS = \sqrt{\frac{1}{M} \sum_{j=1}^{M} \left[f(t_j, \mathbf{x}) - y(t_j) \right]^2} \qquad (9)$$

The value of the RMS shows the quality of the fit. Lower RMS value shows a better fit between the observation data and the model data.

Another important aspect of the nonlinear optimization is the initial guess for the parameters. Since we are dealing with a nonlinear model, initial guesses might lead to a local minimum or a longer iteration time. Thus, sometimes it is better to run the model with different initial guesses.

4. SYNTHETIC EXAMPLES

In this section the sample runs and their outcomes are investigated. In summary, synthetic data is generated using the numerical model developed. Then some of the grid blocks are chosen as observation points and history matching is performed to the pressure data obtained from these points (this is done to mimic observation wells located at various different locations). The aim is to consider the effects of the location of the observation points on the estimated model parameters.

4.1 Closed system with single well in the middle (Case-1)

The first sample run is done with a 101x101 grid reservoir having a production well in the center. The production well has a constant flow rate which is 200 kg/s and there is no aquifer connected to the reservoir.

The initial pressure for each grid blocks is 300. The κ values for each grid block is taken as 4.9×10^5 kg/bar and transmissibilities between each grid block is taken as 5 kg/(bar-s). For the wells created in the system, it is assumed to have no well bore storage and the well transmissibilities (the well index WI) are equal to 5 kg/(bar-s) in order to simplify the case. It is assumed that no recharge source exists that supports the reservoir.

At the end of the simulation run ($t_{end} = 5342$ *days*) the calculated average reservoir pressure is 115.38 bars. The minimum grid cell pressure is 84.05 bars and the maximum grid cell pressure is 117.58 bars.

In Figure 2, the percentage difference of average reservoir pressure with the grid block pressures are given for final time step.

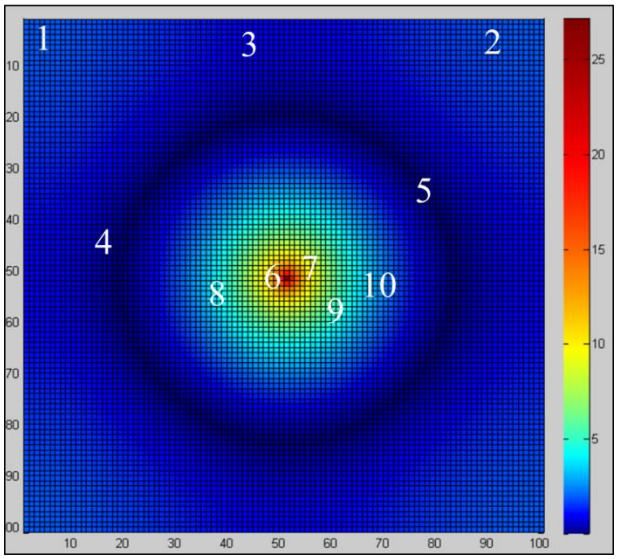

Figure 2: Percentage difference of the grid blocks with the average reservoir pressure in Case-1.

As it can easily be seen the highest difference is in the middle of the reservoir where a production well is active. As we move to the boundaries of the reservoir the pressure difference decreases until where we reach the dark blue region. This region is the place where the difference between the grid block pressures and the average reservoir pressure is minimum. The difference starts to increase as we move further away from the well towards the outer boundaries of the reservoir.

From the output of the simulation run ten arbitrary grids are chosen (indicated by the white numbers in Figure 2). Summary regarding the pressures obtained from these points are given in Table 1.

Table 1: Grid blocks and their pressures at last timestep.

Index	Grid Number	Grid block pressure at t_{end}	Percentage difference between grid block pressures and the average reservoir	Absolute difference between grid block pressures and the average reservoir
1	306	117.566	1.897	2.189
2	9398	117.508	1.847	2.131
3	4649	116.479	0.955	1.102
4	1865	115.387	0.0082	0.0094
5	8043	115.375	-0.0016	-0.0018
6	5101	84.046	-27.15	-31.33
7	5404	101.248	-12.25	-14.13
8	4396	106.921	-7.329	-8.456
9	6318	110.060	-4.608	-5.317
10	6724	112.249	-2.711	-3.128

For this case, it is known that there are 10201 grid blocks with each block having a storage capacity of 4.9×10^5 kg/bar and if we think this reservoir as a one big closed reservoir the total storage capacity will become $5x10^9$ kg/bar. In Figure 3, the schematic of the lumped parameter model used for the history matching can be seen.

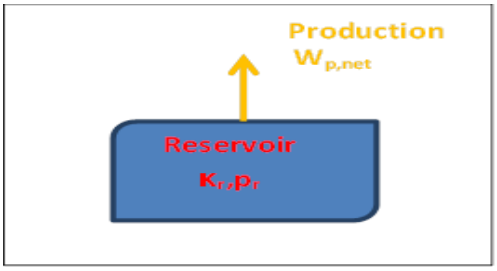

Figure 3: Single tank closed model schematic.

The nonlinear optimization model that was developed is run for pressures obtained from each grid and the matched parameters for these runs are tabulated in Table 2.

Table 2: Nonlinear optimization results for the arbitrary grids in Case-1.

Index	Grid Number	RMS (bar)	Storage Capacity (kg/bar)	Error for κ (%)
1	306	0.619	5.11×10^9	2.20%
2	9398	0.604	5.107×10^9	2.14%
3	4649	0.347	5.055×10^9	1.10%
4	1865	0.079	5.0×10^9	0.01%
5	8043	0.074	5.0×10^9	0.00%
6	5101	13.13	3.815×10^9	-23.70%
7	5404	4.984	4.386×10^9	-12.28%
8	4396	2.755	4.614×10^9	-7.73%
9	6318	1.643	4.75×10^9	-4.99%
10	6724	0.925	4.85×10^9	-3.00%

As it can be seen from the above table, the grids having greater deviations form the average reservoir pressure have less accurate estimates for the storage capacity values. The outputs for storage capacities vary between 3.8×10^9 and 5.1×10^9 kg/bar. Actually this case is showing that the observation well has to be chosen in a region which has less difference with the average reservoir pressure. Again when we look at the RMS values; the run having highest difference has the highest RMS value which indicates that the parameters that provide the history match are not reliable. In Figure 2, Grid 8043is on the dark blue ring region which has nearly an absolute match according to its Error and RMS values. Figure 4 illustrates the pressures observations in Grid 8043 and the matched model's pressures.

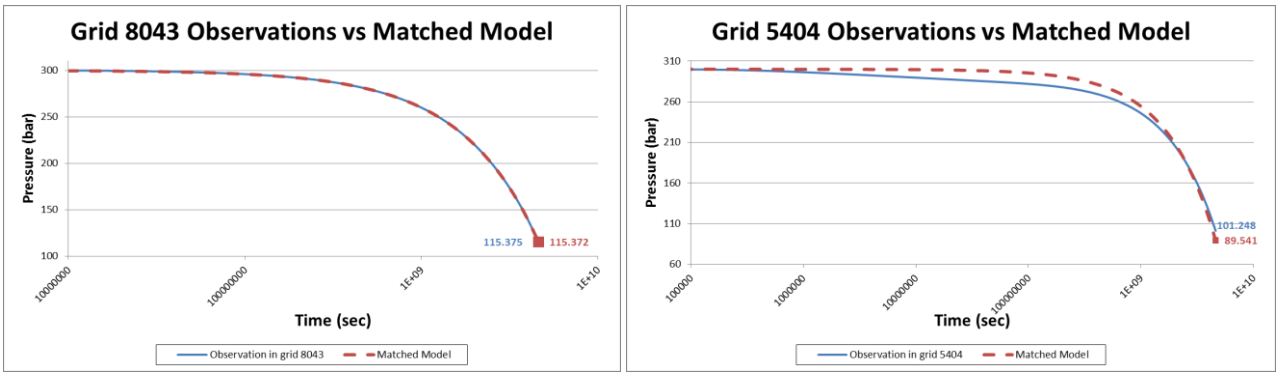

Figure 4 : Comparison of grid observations and matched model pressures (a) grid 8043 (b) grid 5404.

4.2 Open system with single well in the middle (Case-2)

The second sample run is done with a 101×101 grid reservoir having a production well in the center. The production well has a constant flow rate which is 200 kg/s and there is an aquifer connected to the reservoir from left.

Again similar to the previous run, the initial pressure for each grid blocks is 300 bar. The κ values for each grid block are taken as 4.9×10^5 and the transmissibilities between each grid block is taken as 5 kg/(bar-s). The α values between each grid block on the left and the recharge source is taken as 5 kg/(bar-s) as well.

At the end of the simulation run ($t_{end} = 33076$ *days*) the calculated average reservoir pressure is 284.8 bars. The minimum grid cell pressure is 251.83 bars and the maximum grid cell pressure is 299.6 bars.

In Figure 5, the percentage difference of average reservoir pressure with the grid cell pressure is illustrated.

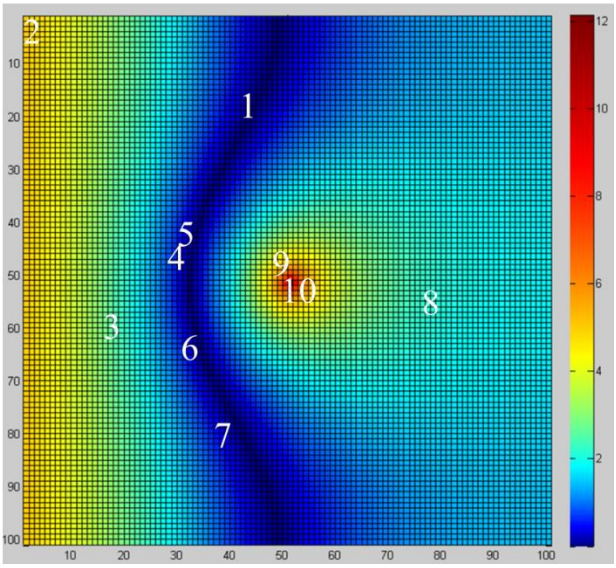

Figure 5: Percentage difference of the grid blocks with the average reservoir pressure in Case-2.

Again for this case, highest difference is in the middle of the reservoir where the production well is active. Also there is a high pressure zone where the aquifer is connected. The region with the least difference is given with the dark blue color..

From the output of the simulation run ten arbitrary grids are chosen (indicated by the white numbers in Figure 5). Summary regarding the pressures obtained from these points are given in Table 3.

Table 3: Grid blocks and their pressures at last timestep.

Index	Grid Number	Grid block pressure at t_{end}	Percentage difference between grid block pressures and the average reservoir pressure	Absolute difference between grid block pressures and the average reservoir pressure
1	4361	284.805	0.001	0.0034
2	1	299.636	5.209	14.83
3	1777	292.229	2.608	7.43
4	3077	285.702	0.316	0.9
5	3275	284.954	0.054	0.15
6	3498	284.668	-0.047	-0.1337
7	4010	283.936	-0.304	-0.866
8	7933	278.561	-2.191	-6.24
9	5200	267.089	-6.219	-17.71
10	5101	251.827	-11.578	-32.97
-	Paverage	284.802	0.0	0.0

Similar to the previous case, when the whole reservoir is thought of as a single big tank the storage capacity of this tank will be $5x10^9$ kg/bar. For this case there is an aquifer connected from the west of the reservoir. The lumped parameter model that is used ,n the history matching process is given in Figure 6.

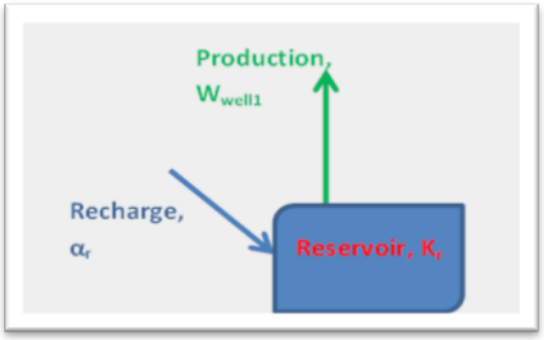

Figure 6 : Single tank open model schematic.

In the inverse modeling, the values for storage capacity (κ) and recharge index between aquifer and the reservoir (α) is determined as if the system is represented by a single tank open model. The results are tabulated in the Table 4.

Table 4: Nonlinear optimization results for the arbitrary grids in Case-2.

Index	Grid Number	RMS (bar)	Storage Capacity (kg/bar)	Error κ (%)	Recharge Index (kg/bar-s)
1	4361	0.09	5.00×10^9	0.0%	13.21
2	1	0.07	8.46×10^9	69.2%	854.69
3	1777	0.09	7.80×10^9	55.9%	26
4	3077	0.29	3.39×10^9	-32.3%	14.27
5	3275	0.3	3.24×10^9	-35.2%	13.56
6	3498	0.27	3.41×10^9	-31.8%	13.27
7	4010	0.21	3.75×10^9	-25.0%	12.6
8	7933	0.07	3.91×10^9	-21.8%	9.32
9	5200	2.45	2.70×10^8	-94.6%	6.73
10	5101	5.01	8.02×10^6	-99.8%	5.06
-	Paverage	0.05	5.00×10^9	0.0%	13.21

From the above table it can easily be seen that, unlike the closed system, most of the grids have errors higher than 20%. The only grid that has error less than 20% is Grid Cell 4361. From Figure 5, it can be seen that this grid cell is in the region of dark blue. Again higher the difference between the grid pressure and the average reservoir pressure, higher the error in the matched parameters. The matched models and pressure observations for Grid 4361 and Grid 5200 are shown in Figure 7.

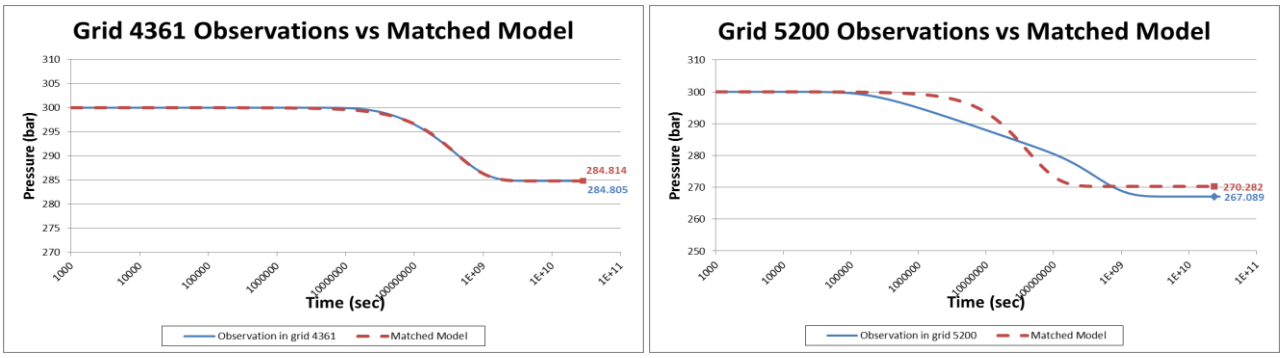

Figure 7 : Comparison of grid observations and matched model pressures (a) grid 4361 (b) grid 5200.

As the RMS indicates the match is very good between the lumped parameter model and the pressure obtained from grid block 4361. On the other hand, the matched model and the observations in grid 5200 shows great deviation.

4.3 Discussion

In this subsection a numerical experimentation is carried out for the effects of observation well locations on the estimated model parameters. The two cases considered here are given for idealized simple geometries. As a result of the two cases, we may conclude that the location of the observation wells, from which we obtain pressures to be matched with lumped parameter models, are indeed very important and that if the observation well pressures do not correctly represent the average reservoir pressures, the determined model

parameters may contain large errors. Based on the above two cases we may also conclude that the errors introduced in determining the model parameters become more pronounced when open systems are considered so that the solution of the proper observation well requires greater attention.

6. CONCLUSION AND FUTURE WORK

This paper presents the preliminary results of an ongoing study. The following conclusions are obtained until now:

- A numerical model is developed and the output of the model is validated with known analytical and numerical models.
- An inverse model is developed for the inference of model parameters. The models used in this study are lumped parameter models.
- Several case studies have been completed to study the effects of the location of observation wells for history matching to be used with lumped parameter models.
- More complex and realistic cases with multiple wells will be considered in the future for a better understanding of the errors involved.
- A relationship between model parameters and actual petrophysical properties (such as permeability, porosity and etc.) of the reservoir will be considered.

REFERENCES

Alkan, H., and Satman, A. (1990). A New Lumped Parameter Model for Geothermal Reservoirs in Presence of Carbon Dioxide. *Geothermics*, **19**, No 5, 469-479.

Axelsson, G. (1989). Simulation of Pressure Response Data from Geothermal Reservoirs by Lumped Parameter Models. *Proceedings*, 14th Workshop on Geothermal Reservoir Engineering, Stanford Univeristy, 257-263.

Castanier, L.M., Sanyal, K.S., Brigham, W.E. (1980). A Practical Analytical Model for Geothermal Reservoir Simulation. *50th Annual California Regional Meeting of SPE*, Los Angeles, California, April 9-11, SPE 8887.

More, J.J. (1978). The Levenber-Marquardt Algorithm: Implementation and Theory. *Numerical Analysis*. 105-116.

Olsen, G. (1984). Depletion Modeling of Liquid Dominated Geothermal Reservoirs. *Technical Report*, SGP-TR-80, Stanford Geothermal Program, Stanford Univeristy.

Onur, M., Sarak, H., Türeyen, Ö.İ., Çınar M., Satman, A. (2008). A New Non-isothermal Lumped-parameter Model for Low Temperature Liquid Dominated Geothermal Reservoirs and Its Applications. *Proceedings*, 33rd Workshop on Geothermal Reservoir Engineering, Stanford University, Stanford, January, 28-30.

Sarak, H. (2004). Düşük Sıcaklıklı Jeothermal Rezervuarlar için Boyutsuz Rezervuar Modelleri. *Ph.D.thesis*, ITU.

Sarak, H., Onur, M., Satman, A. (2005). Lumped-parameter Models for Low Temperature Geothermal Reservoirs and Their Applications. *Geothermics*, **34**, 728-755.

Schilthuis. R.J. (1936). Active Oil and Reservoir Energy. Trans. *AIME*, vol. **118**, pp. 33-52.

Türeyen, Ö.İ., Onur, M., Sarak, H. (2009). A Generalized Nonisothermal Lumped-parameter Model for Liquid Dominated Geothermal Reservoirs. *Proceedings*, 34rd Workshop on Geothermal Reservoir Engineering, Stanford University, Stanford, February, 9-11.

Türeyen, Ö.İ., Akyapı, E. (2011). A Generalized Nonisothermal Tank Model for Liquid Dominated Geothermal Reservoirs. *Geothermics*, **40**, 50-57.

Türeyen, Ö.İ., Sarak, H., Onur, M. (2007). Assessing Uncertainty in Future Pressure Changes Predicted by Lumped-Parameter Models:A Field Application. *Proceedings*, 32nd Workshop on Geothermal Reservoir Engineering, Stanford University, Stanford, January, 22-24.

Whiting, R.L., Ramey, H.J.Jr. (1969). Application of Material and Energy Balance to Geothermal Steam Production. *Journal of Petroleum Technology*, July, 893-900.